Applied Catalysis B: Environmental 154–155 (2014) 259–266

Contents lists available at ScienceDirect

Applied Catalysis B: Environmental

journal homepage: www.elsevier.com/locate/apcatb

Revealing the degradation intermediates and pathways of visible light-induced NF-TiO_2 photocatalysis of microcystin-LR

Joel Andersen [a], Changseok Han [a], Kevin O'Shea [b], Dionysios D. Dionysiou [a,*]

[a] Environmental Engineering and Science Program, University of Cincinnati, Cincinnati, OH 45221-0012, USA
[b] Department of Chemistry and Biochemistry, Florida International University, Miami, FL 3319, USA

ARTICLE INFO

Article history:
Received 2 December 2013
Received in revised form 7 February 2014
Accepted 14 February 2014
Available online 22 February 2014

Keywords:
Microcystin-LR intermediates
Visible light
TiO_2 photocatalysis

ABSTRACT

The effect of using only visible light to induce nitrogen- and fluorine-doped titanium dioxide (NF-TiO_2) photocatalysis of degradation products of microcystin-LR (MC-LR), the most common problematic cyanotoxin, was explored by looking at the intermediate degradation products. Although the degradation mechanisms and products of conventional UV-based TiO_2 photocatalysis of MC-LR have been well elucidated, the same is not true for visible light-based TiO_2 photocatalysis. The results of LC/MS^2 (and in one case LC/MS^3) indicated that the intermediates are not drastically altered in comparison to traditional TiO_2 photocatalysis using UV light. The data hint that the degradation is driven by hydroxyl radicals, as is UV-based TiO_2 photocatalysis, although the mechanism for producing hydroxyl radicals is unclear since studies indicate drastically slower kinetics for visible light-based photocatalysis of MC-LR. Notably, the data indicate that visible light-induced NF-TiO_2 photocatalysis degraded the portion of MC-LR that is responsible for biological toxicity. As a result of this, it was concluded that doping TiO_2 with nitrogen and fluorine is an effective method for increasing utilization of visible light while degrading MC-LR in water, although it should still be noted that degradation kinetics are still slower than UV-based TiO_2 photocatalysis.

1. Introduction

In 2009, the United States Environmental Protection Agency (EPA) published the third edition of their Contaminant Candidate List (CCL3) [1]. The goal of CCL3 was to identify chemicals and microbes that met the following criteria: (1) The chemical was not already subject to national regulation, (2) The chemical had been observed in, or was reasonably expected to be present in, public water systems, and (3) The chemical potentially falls within the scope of the Safe Drinking Water Act (SDWA). In CCL3, the EPA identified 104 chemicals and 12 microbes as candidates. Some of these candidates consist of similar chemicals that have been grouped together. Cyanotoxins are one such group. These potent toxins are naturally produced by algae in fresh and brackish waters. There are several dozen congeners of cyanotoxins, but the EPA explicitly highlighted three of them as being of the greatest concern: anatoxin-a, microcystin-LR (MC-LR), and cylindrospermopsin. Of these three toxins, indeed, of all known cyanotoxins, MC-LR is the most frequently occurring cyanotoxin and is also among the most toxic [2]. This being the case, MC-LR is a worrisome environmental contaminant and is worthy of further attention.

Microcystin-LR is produced by several members of a group of algae called cyanobacteria. Occurrences of cyanobacterial harmful algal blooms, often referred to as Cyano-HABs, are a growing threat worldwide [3]. Cyanobacteria cells produce and retain MC-LR until they are ruptured, at which point the toxin can be released into the surrounding aquatic environment. Collapse of a Cyano-HAB can quickly lead to high levels of MC-LR. Following release into the environment, MC-LR is a persistent molecule [4]. The stability is due in large part to the cyclic heptapeptide structure held together by strong amide bonds (see Scheme 1 for details on the structure of MC-LR) [4]. Note that Scheme 1 highlights several moieties, including Adda, Mdha, and various other amino acids. The toxicity associated with MC-LR is largely attributable to the Adda chain [5]. Removal of the Adda side chain or isomerization about the hydrophobic Adda C_6–C_7 bond (see Scheme 1), from *trans* to *cis*, eliminates the associated toxicity. This *trans* to *cis* photoisomerization requires UV C light (100 nm ≤ λ ≤ 280 nm) and does not occur under visible light [5].

Numerous reports have appeared on potential technologies for removing and/or detoxifying MC-LR. These technologies include conventional chlorine- and permanganate-based treatments [6],

* Corresponding author at: Department of Biomedical, Chemical and Environmental Engineering, 705 Engineering Research Center, University of Cincinnati, Cincinnati, OH 45221-0012, USA. Tel.: +1 513 556 0724; fax: +1 513 556-2599.
E-mail address: dionysios.d.dionysiou@uc.edu (D.D. Dionysiou).

http://dx.doi.org/10.1016/j.apcatb.2014.02.025
0926-3373/

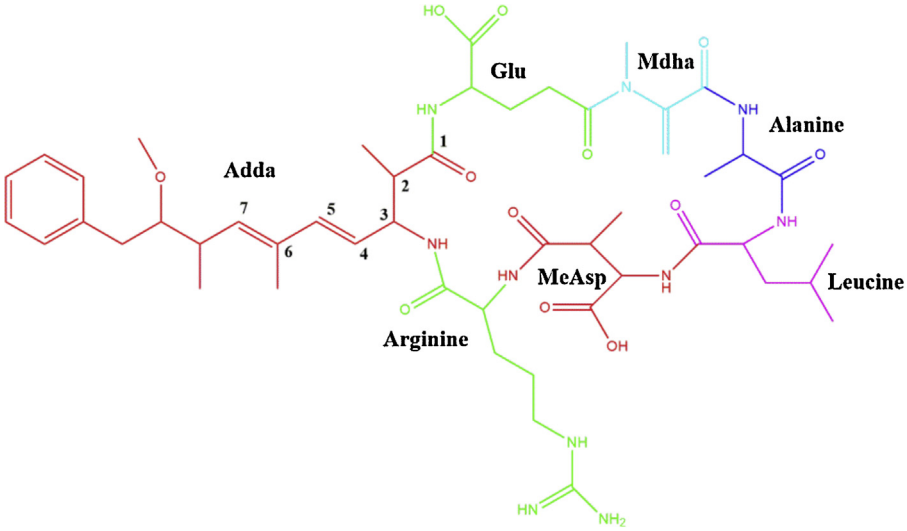

Scheme 1. Structure of microcystin-LR.

ozonation [7], phototransformation [8], and advanced oxidation technologies (AOTs) such as titanium dioxide (TiO_2) photocatalysis [9]. In comparison to other treatments, TiO_2 photocatalysis demonstrated great promise. Antoniou et al. reported the reaction pathways and intermediate degradation products produced by conventional UV-based TiO_2 photocatalysis [10]. One of the primary sites of oxidative attack during UV-based TiO_2 photocatalysis is at the Adda side chain. Since the Adda side chain is critical to biological activity, altering it is a key step to reducing the biological activity. The same study by Antoniou et al. revealed that the photocatalytic oxidative attacks of UV-based TiO_2 occurred at the phenyl, methoxy, and alkene functional groups of the Adda moiety. To a lesser extent, an additional site included the carbon-carbon double bond on Mdha. More specifically, Antoniou and colleagues observed that the intermediates were consistent with attacks by hydroxyl radicals (•OH). Although generation of •OH during UV-activated TiO_2 photocatalysis is well established [11,12], the degradation mechanism of NF-TiO_2 activated by visible light without UV light (VLA-TiO_2) is under active investigation. Although effective, illuminating TiO_2 photocatalytic material with UV light is costly; thus, development of a photocatalyst that can be activated in the visible range has a huge economic advantage. Extending photoexcitation into the visible light range allows the catalyst to use a larger portion (~45%) of the sun's electromagnetic radiation as opposed to being limited to the ultraviolet light portion (~4-5%) [13]. Such activation is possible through the use of dopants like nitrogen and fluorine to alter the band gap of the material [13]. However, doping changes the relative positions of the valence and conduction bands, which can in turn influence production of reactive oxygen species and subsequent degradation pathways. Visible light-activated TiO_2 has tremendous potential as a sustainable water treatment process; however, the degradation pathways and degradation products may vary significantly from UV-based TiO_2 photocatalysis. Therefore, it is apropos and timely to determine these factors associated with VLA NF-TiO_2 photocatalysis.

2. Experimental

2.1. Safety

An Advance Sterilchem GARD III Class II Biological Safety Cabinet (The Baker Co.) was used in the preparation of all MC-LR solutions. The reactor described in Section 2.4: Reactor Design was contained within the biological hood throughout the experiments.

2.2. Materials

MC-LR was purchased as a solid from Calbiochem (Gibbstown, NJ). The solid (0.5 mg, 96.4% purity) was stored in a freezer at –20 °C. Addition of 1 ml of autoclaved Milli-Q water produced a 500 ppm stock solution. This solid was allowed to dissolve over a two day period and was vortexed for 1 min each day. On the day of use, the stock solution was vortexed for a minimum of 20 s. For a control experiment, an un-doped TiO_2, Hombikat UV 100, was used (Sachtleben Chemie GmbH, D-47184 Germany).

2.3. NF-TiO_2 preparation and characterization

The NF-TiO_2 films were prepared following a sol–gel method previously disclosed by Pelaez et al. [13]. Accordingly, the sol–gel was prepared with titanium (IV) tetraisopropoxide (TTIP, 97%, Aldrich), Zonyl-FS 300 (Fluka), isopropanol (99.8%), glacial acetic acid, and anhydrous ethylenediamine, the last three of which were purchased from Fisher Scientific. To obtain a powder from the NF-TiO_2 sol–gel, a thin layer of sol–gel was deposited into a borosilicate glass petri dish. The dish was subsequently calcined in a programmable Paragon furnace (HT-22-D, Thermcraft) at 400 °C for 120 min. After 30 min the dish was removed and allowed to naturally cool to room temperature. From the resulting powder, a 1 g/L solution was prepared using SQ water. This stock solution was sonicated for 20 min after preparation and for 10 min prior to use.

2.4. Reactor design

The volume of the reaction solution was 10 ml with 0.5 g/L of photocatalyst and 5 ppm MC-LR. The solution was transferred to a 60 mm diameter borosilicate glass petri dish. Sitting atop a stir plate, the solution was magnetically stirred throughout the experiment. This solution was irradiated by two 15 W fluorescent lamps (Cole-Parmer); UV radiation was filtered out using a UV filter (UV420, Opticology). The spectrum of the light reaching the sample contains no ultraviolet light, and it can be seen in Supplementary Fig. S1. Initial removal of MC-LR from the solution is the result of physical adsorption to the photocatalyst and visible light activation of the photocatalyst. Samples were taken in 100 μL amounts. To prevent the photocatalyst particles from entering the sensitive analytical instrumentation, each sample was filtered with a Whatman® Mini-UniPrep® syringeless filter with slit septa (PTFE, 0.2 μm). Prior to filtering, each sample was diluted with 100 μL of methanol.

2.5. High-performance liquid chromatography (HPLC) analysis

High-performance liquid chromatography was used to determine the decrease in MC-LR concentration over time. An Agilent 1100 Series quaternary liquid chromatograph equipped with a C_{18} Discovery (Supelco) column (150 mm × 2.1 mm, 5.0 μm particle size) was used. Two components made up the mobile phase. Component A was 0.05% trifluoracetic acid (TFA) in water, and component B was 0.05% TFA in acetonitrile. The isocratic flow consisted of 60% A and 40% B. The flow rate was set to 0.2 mL/min, the injection volume was 20 μL, and 238 nm was used as the wavelength for detection using a photodiode array detector. The temperature of the column was maintained at 40 °C. MC-LR eluted after approximately 5.3 min under these conditions.

2.6. LC/MS analysis

Liquid chromatography for structure elucidation was performed using an Agilent 1100 Binary Liquid Chromatograph. The injection volume was 10 μL. The column, which was used at room temperature, was a Waters XTerra MS C_8 Column (150 mm × 2.1 mm, 3.5 μm particle size). The flowrate was 0.3 ml/min. A two-component solvent with a gradient method was used. Component A consisted of 0.1% formic acid in water, and Component B consisted of 0.1% formic acid in methanol. The gradient began at initial conditions of 15% B, followed by a 10 min linear ramp to 25% B, another 10 min linear ramp to 40% B and finally a 15 min linear ramp to 80% B. At all times, the remaining fraction of the mobile phase consisted of Component A. The column was allowed to re-equilibrate to initial conditions for 10 min between injections for a total analysis cycle time of 45 min.

A Scientific LTQ XL ion trap mass spectrometer was utilized for the MS, MS^2, and MS^3 determination of the reaction by-products. Positive ion electrospray ionization (ESI) was used and full-scan mode (*m/z* 300–1200) was used to obtain MS. The auxiliary gas was at 25 (unitless), ESI sheath gas was at 80 (unitless), and the capillary temperature was 300 °C. The source voltage was 4.0 kV. The instrument was tuned with MC-LR to achieve maximum sensitivity. For full-scan MS/MS analyses, the selected precursor ions were isolated with an isolation width of 1 Da. The collision induced dissociation (CID) energy for all MS^2 spectra was a normalized value of 16. The normalized CID energies for the second transition in MS^3 were 22 for fragment *m/z* 1007.5 and 25 for fragment *m/z* 793.4, both of which were produced during the fragmentation of intermediate *m/z* 1025.5.

3. Results and discussion

3.1. HPLC analysis of the MC-LR concentration

The removal of MC-LR over the 8-h period of irradiation is shown in Fig. 1. As mentioned earlier the significant amount of removal during the first hour is likely in large part due to adsorption. However, subsequent degradation over the remaining time is the result of visible light activation of the NF-TiO_2 photocatalyst. The intermediate products appearing in samples irradiated with visible light were monitored for up to 8 h of visible light irradiation.

3.2. LC/MS results

For product analyses, only signal peaks with a signal-to-noise ratio greater than or equal to three were considered. Additionally, peaks present in the initial sample or blank were not considered unless the relative peak area changed by at least a factor of two.

Additionally, the legitimacy of the experimental setup was confirmed by a control experiment using conventional TiO_2. In this control experiment, no intermediates were observed during LC/MS analysis. The absence of intermediates confirms that any intermediates that appear in subsequent experiments with nitrogen- and fluorine-doped TiO_2 can be attributed to visible-light activation of the material. A comparison of the UV–vis absorbance of the reference photocatalyst and filtered radiation spectrum is available in Supplementary Fig. S2.

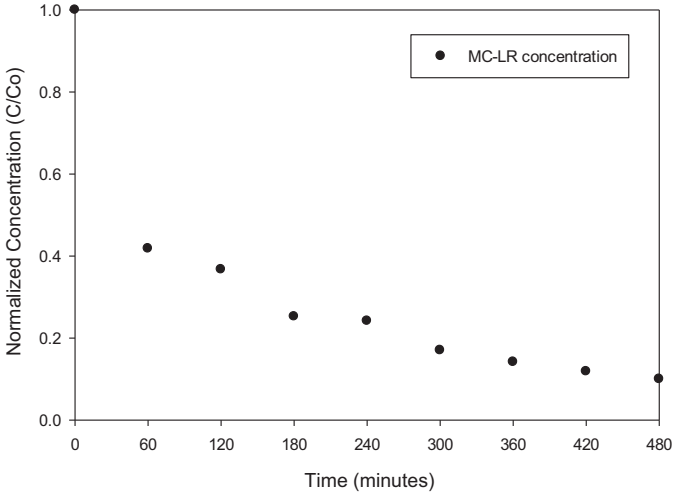

Fig. 1. Removal of MC-LR ($[MC\text{-}LR]_0$ = 5 ppm) over 8 h of visible light irradiation in the presence of 0.5 mg/L NF-TiO_2 photocatalyst.

Analysis of the LC/MS results indicated ten different peaks. The unknown peaks and the MC-LR peak are summarized in Table 1 according to *m/z* value. The presence of multiple peaks for a single *m/z* value can occur as a result of constitutional isomers. Since the difference in polarity between two constitutional isomers is often minimal, separation is difficult and a single peak may represent a number of multiple constitutional isomers. Also, note the close proximity of some retention times that are within a few mass units. This must be taken into account when performing LC/MS/MS analyses since MC-LR has *m/z* 996.5 $[M + H + 1]^+$ and *m/z* 997.5 $[M + H + 2]^+$ isotopic peaks at approximately 50% and 25% abundances. Hence, the isolation width must be carefully selected for peaks such as *m/z* 1027.5 to avoid mixed spectra (e.g., interference from the *m/z* 1025.5 +2 Da isotope). Of the 10 product peaks in Table 1, nine had *m/z* values identical to previously observed intermediates [10]. Despite identical *m/z* values, LC/MS/MS interpretation of all intermediates was still necessary due to the likelihood of constitutional isomers. Of the observed spectra, only one did not match a previously observed intermediate.

3.3. LC/MS/MS interpretation

Structure elucidation of MC-LR products of advanced oxidation techniques using LC/MS/MS has been well covered in literature [10,14]. In general, small losses of NH_3, H_2O, CO, and CO_2 occur,

Table 1
Observed intermediates and corresponding retention times.

m/z	No. of peaks	Retention times (min)
795.4	1	2.6
835.4	1	3.6
995.5	1	20
1011.5	4	12.7, 14.8, 15.8, 17.3
1025.5	1	18.4
1027.5	1	13.2
1029.5	1	12.5
1045.5	1	14.2

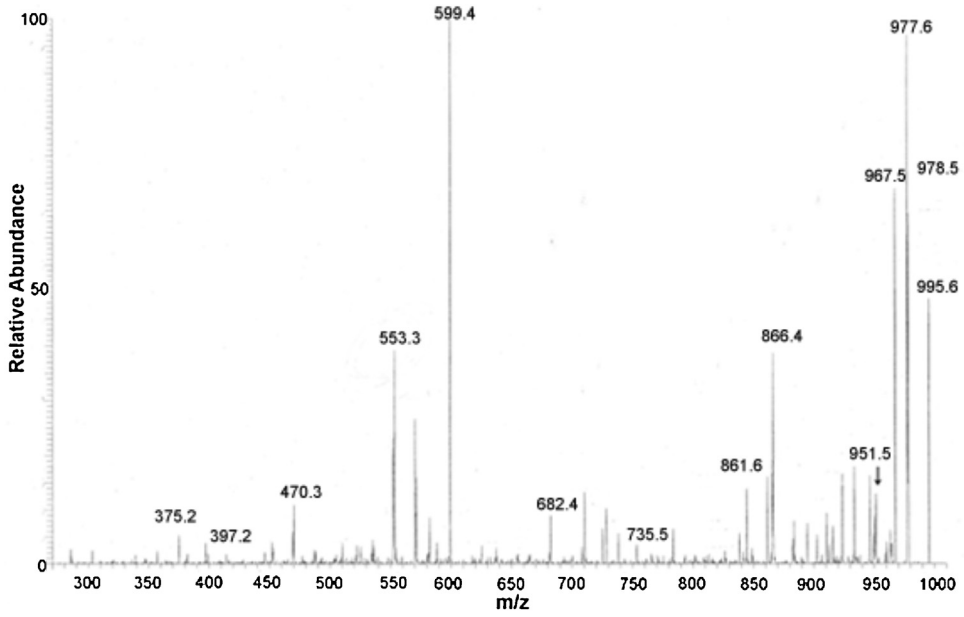

Fig. 2. LC/MS^2 of MC-LR.

but larger losses from the $[M+H]^+$ ion result from losses of intact amino acids. It is generally possible to observe fragments corresponding to a loss of consecutive amino acids, beginning with a loss of MeAsp and proceeding in a counterclockwise fashion around the ring [14]. This behavior is outlined in Fig. 2, which contains the MS^2 of MC-LR. Although some of these fragments could be produced by losses of isobaric amino acids (e.g., MeAsp and D-Glu both have a mass of 129 Da), the approximation above is reliable enough for the ensuing analyses. Select fragments are especially useful as diagnostic fragments. The presence, lack, or alteration of these fragments is critical to identifying the chemical structure of an unknown microcystin derivative. For example, if the *m/z* 599 fragment

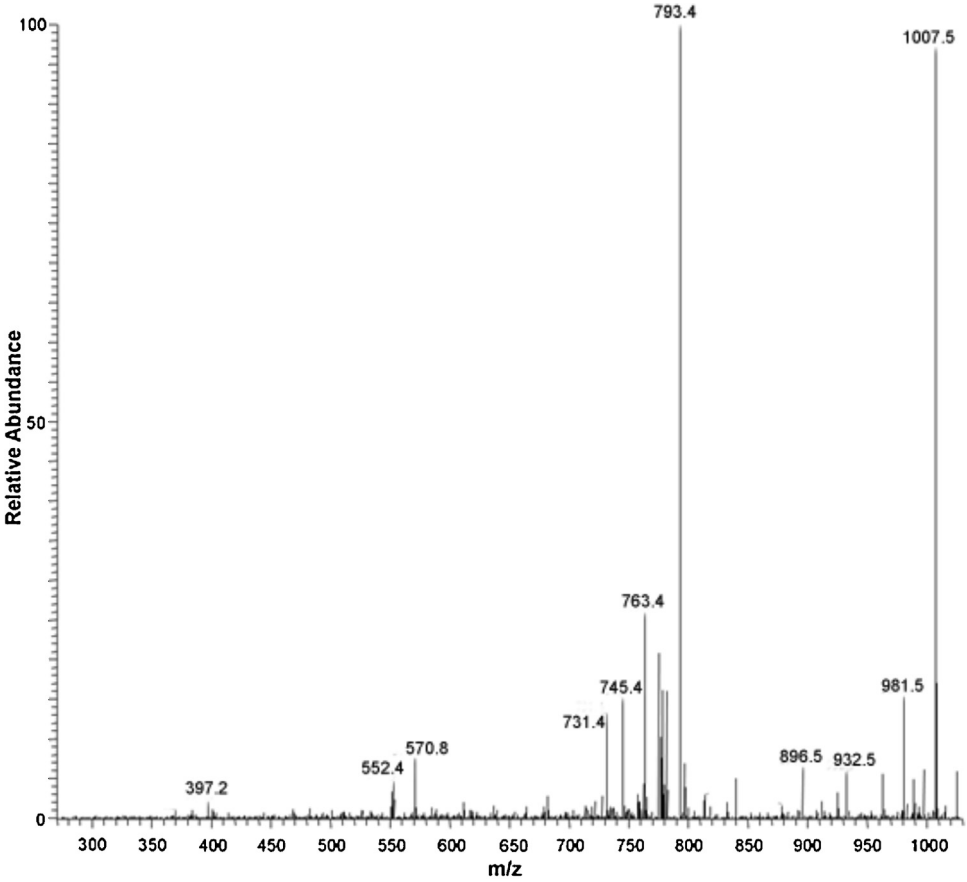

Fig. 3. LC/MS^2 of novel intermediate *m/z* 1025.5.

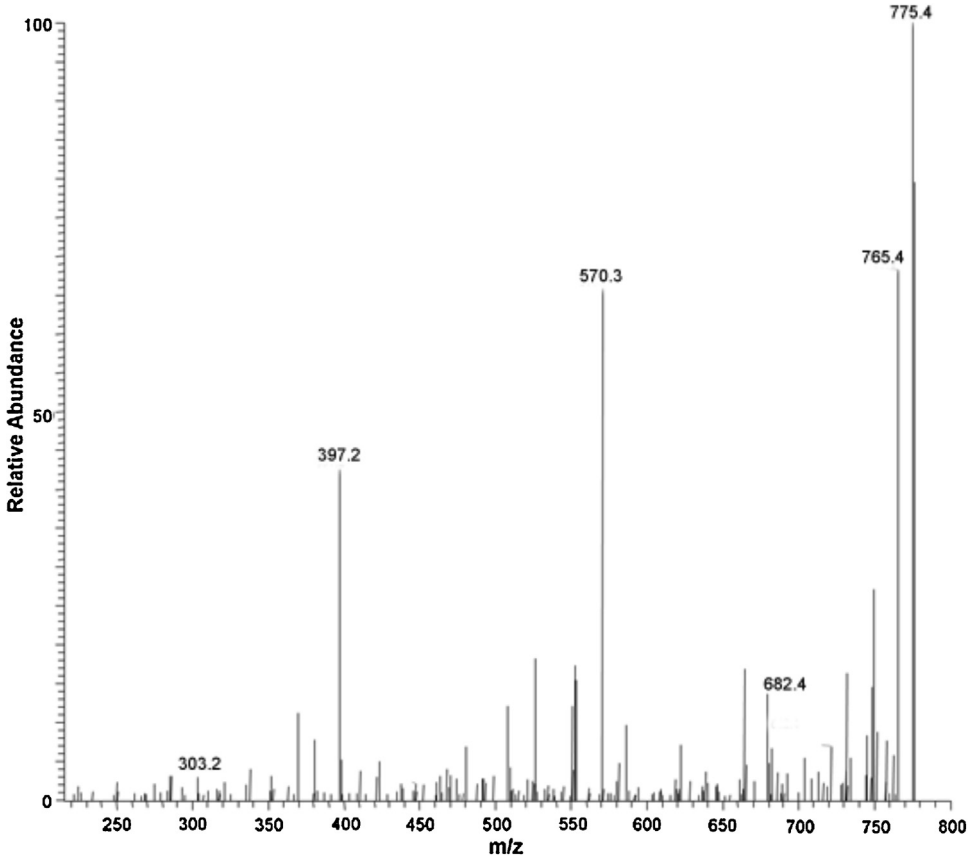

Fig. 4. LC/MS^3 targeting *m/z* 793.4 of 1025.5.

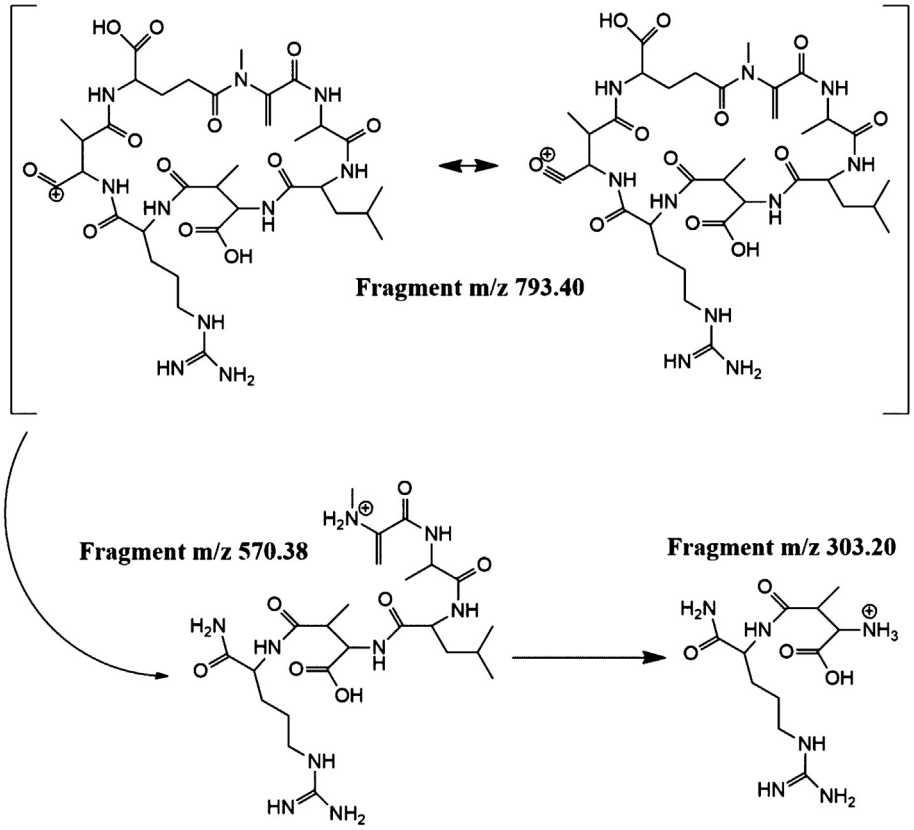

Scheme 2. Fragmentation of *m/z* 793.4 during LC/MS^3.

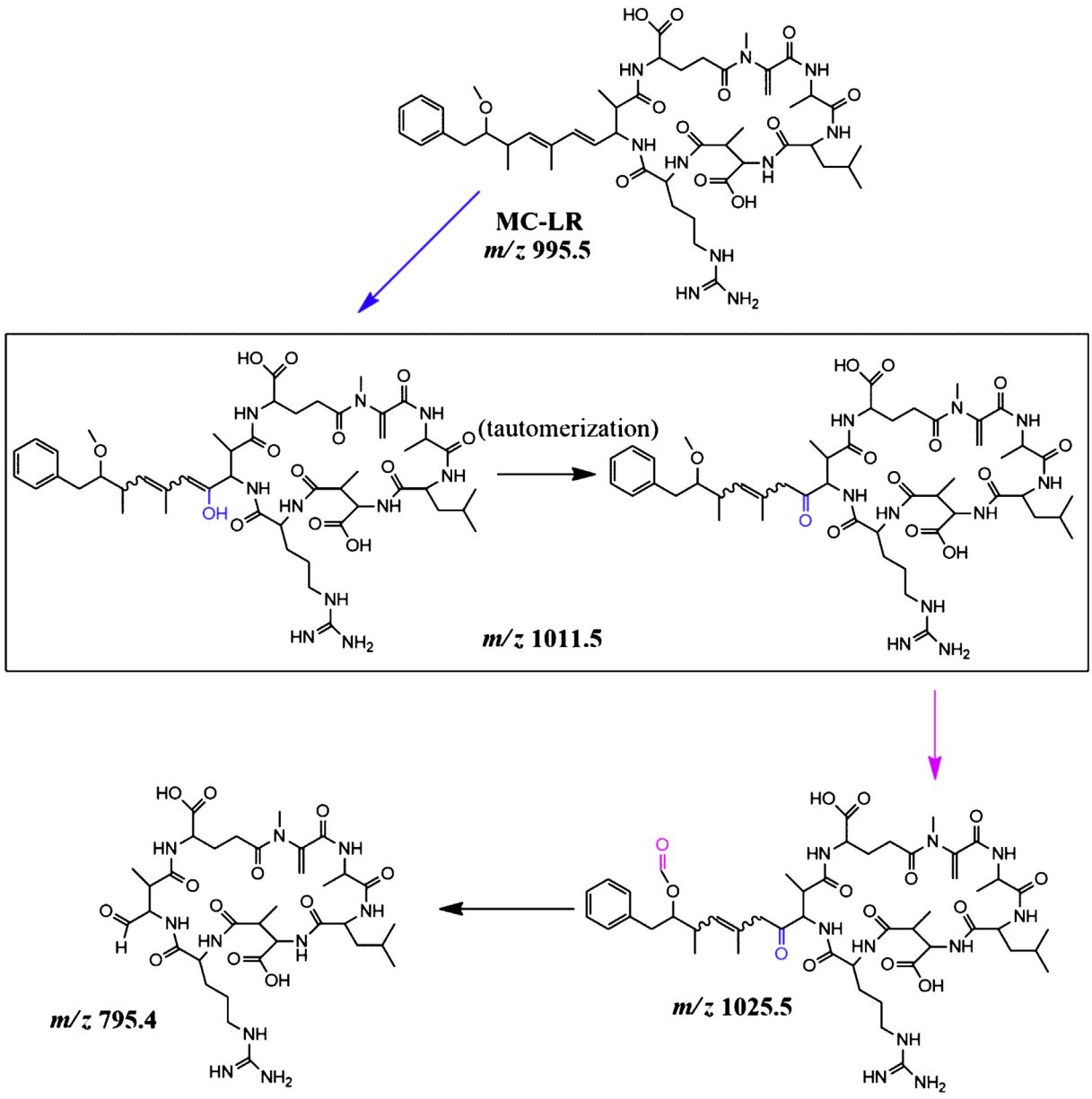

Scheme 3. Degradation pathway involving the novel intermediate.

disappears and an *m/z* 615 fragment appears, then immediately one should suspect hydroxylation (+16 Da) of the *m/z* 599 fragment. One way to further define the site of attack is to exclude the phenyl ring as a possible site if a loss of 134 Da occurs (for example, *m/z* from 995 to 861). This is a neutral loss that occurs as a result of rearrangement involving the ring and methoxy groups, producing what is known as the 134Adda molecule. Along with that, a peak at *m/z* 375.1 can represent either [Arg-Adda-Glu-H-(NH_3)-(134Adda)] or [MeAsp-Arg-Adda-H-(NH_3)-(134Adda)], both of which provide further evidence of an unaltered phenyl ring on the Adda moiety. However, Microcystin-LR derivatives do not invariably fragment in this manner. For example, the alteration of functional groups on the Adda side chain can drastically alter the fragmentation pattern.

An example of one such alteration is apparent in the MS^2 spectrum of the *m/z* 1025.5 intermediate (MC-LR + 30 Da), as shown in Fig. 3. This intermediate is the novel intermediate observed in this study. The *m/z* 599 fragment is no longer present, but no correlated peak (e.g., *m/z* 599 + 30 Da) appeared to determine the change in mass. The closest possible peak is at *m/z* 611, but an increase of 12 Da does not make an obvious connection with the *m/z* 599 peak. Additionally, only one other diagnostically useful fragment is available to further elucidate the structure. This fragment, *m/z* 397.3, which is also present in the fragmentation of MC-LR, consists of one of two possible sequences of amino acids. It could be either [Mdha-Ala-Leu-MeAsp-H]$^+$ or [Glu-Mdha-Ala-Leu-H]$^+$. Regardless of the true sequence, the presence of this fragment does imply that one possible site of attack on MC-LR, the Mdha amino acid, remained intact and unaffected. As a result of this, the Mdha double bond can be ruled out as the location of any modifications leading to the +30 Da deviation from the mass of MC-LR.

At this point, it is clear that the common diagnostic fragments cannot yield any structural identification for the unidentified compound. However, the disappearance of many diagnostic fragments likely corresponds to the appearance of the base peak ion observed in the spectrum at *m/z* 793.4, which corresponds to [M + H – 232]$^+$. This loss of 232 Da does not correspond to any clear combination of amino acids. Therefore, to continue identifying this unknown, it is

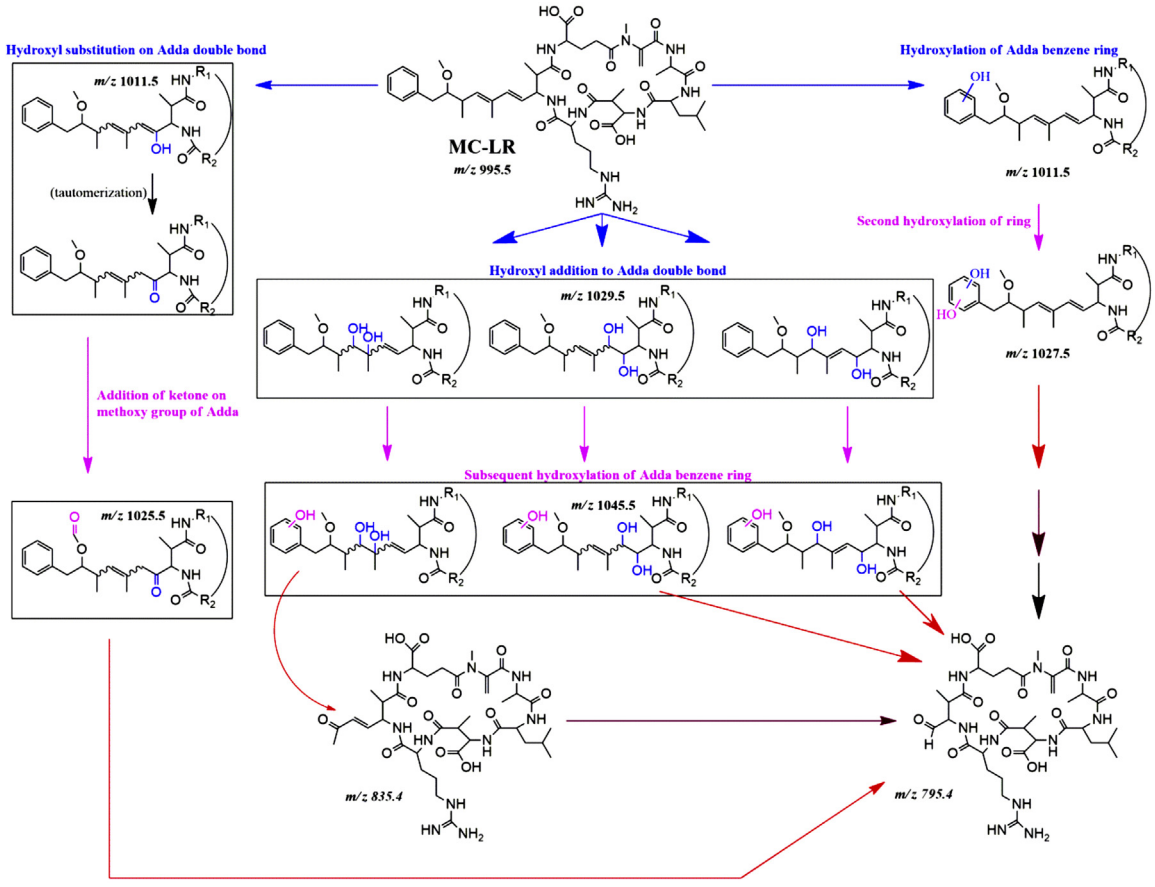

Scheme 4. Summary of VLA NF-TiO_2 degradation pathways.

reasonable to assume that the fragment appears due to fragmentation originating on the Adda chain. This suspicion is confirmed by MS^3, targeting the *m/z* 793.4 fragment of the *m/z* 1025.5 intermediate. The spectrum produced by the LC/MS^3 analysis is available in Fig. 4. The ensuing fragmentation pattern of the *m/z* 793.4 fragment provides comprehensive evidence for structure elucidation. Fragments *m/z* 570.3 and *m/z* 682.4 correspond to intact [Mdha-Ala-Leu-MeAsp-Arg-H]$^+$ and [Glu-Mdha-Ala-Leu-MeAsp-Arg-H]$^+$ sequences, respectively. To determine the remainder of the structure, the mass difference between MC-LR (*m/z* 995.5) and *m/z* 1025.5 can be taken into account. A difference of 30 Da may correspond to the conversion of the methoxy group to an aldehyde (although not found in the present study, this conversion was reported by Antoniou et al. on the *m/z* 1009 intermediate when using UV light TiO_2 photocatalysis [10]) after a hydroxyl substitution. This hydroxylation could occur on either the Adda phenyl group or the Adda double bonds since the change in molecular weight is the same. Note, however, that substitution of a hydroxy functional group in place of a hydrogen atom on the diene double bonds produces keto-enol tautomers whose equilibrium lies essentially in the keto form. In general, keto forms are significantly more stable than their enol counterparts unless there exists significant potential for intramolecular hydrogen bonding. That potential not being present in this molecule, the equilibrium will vastly favor the keto form.

Moving forward, careful analysis leads to the complete determination of structures for the unique LC/MS^3 fragments of the *m/z* 793.4 fragment (Scheme 2). Assuming substitution of a hydroxyl group for the hydrogen on one of the diene double bonds (resulting in rapid tautomerization to the keto form), one can justify the fragmentation of the derivative that produces the unconventional *m/z* 793.4 fragment. As Scheme 2 demonstrates, the keto form of fragment *m/z* 793.4 allows for the presence of two resonance structures. As such, molecular orbital theory predicts the delocalization of neighboring electrons, stabilizing the positively charged, empty p orbital. This delocalization explains the significant stability of the ion suggested by its presence as the base peak in the spectrum of the *m/z* 1025.5 intermediate. Taken together, this fragment's proposed structure and the LC/MS/MS of *m/z* 1025.5 indicate that the hydroxyl substitution occurs on the C_4 carbon of the Adda chain. It is also worth noting that a similar unconventional fragment does not occur in the spectrum corresponding to hydroxyl addition on the Adda double bond (one of the *m/z* 1011.5 constitutional isomers) when the methoxy group remains intact.

3.4. Degradation pathways

The novel intermediate (*m/z* 1025.5) fits neatly into a previously established degradation pathway. The VLA-TiO_2 analog degradation pathway is described in Scheme 3. It is proposed that first hydroxyl substitution of the C_4 carbon on the Adda chain occurs (*m/z* 1011.5), followed by conversion of the methoxy group to an aldehyde (*m/z* 1025.5). Subsequent to these oxidative transformations, the Adda chain is cleaved at the C_4 carbon (*m/z* 795.4). This degradation pathway suggests the loss of toxicity of MC-LR during the photocatalytic transformation of MC-LR by NF-TiO_2 under visible light [10].

In total, VLA-TiO_2 produced ten peaks corresponding to various intermediates. Nine of these peaks contained intermediates that had been identified in previous research. All intermediates are compiled into three proposed degradation pathways in Scheme 4. These three pathways overlap with those proposed previously by

Table 2
Appearance of the intermediates over the 8-h irradiation period.

Time (min)	Intermediate (*m/z*) appearance
60	795.4, 1011.5 (ring), 1027.5, 1029.5
120	1045.5
180	835.4
240	–
300	1025.5
360	–
420	–
480	1011.5 (double bond)

Antoniou and colleagues. The previously discussed pathway from Scheme 3 is contained on the left-hand side of Scheme 4, and the other two pathways consist of simply multiple hydroxylations of MC-LR's Adda amino acid. This tendency results from the oxidative reactive oxygen species' electrophilicity towards the conjugated carbon-carbon double bonds and phenyl group. Both of these sites are areas of high electron-density. Although the intermediates reported herein are consistent with oxidation by hydroxyl radical, the kinetics of visible light-activated NF-TiO_2 are significantly slower than UV-activated NF-TiO_2. One justification for these observations is the possible production of hydroxyl radical through an indirect mechanism. One such indirect pathway for hydroxyl radical generation that has been observed in conventional TiO_2 can be seen in Reaction Scheme 1 [15]. It is possible that the formation mechanism of hydroxyl radical shifts from direct reduction to the indirect mechanism described in Reaction Scheme 1. Hamilton and colleagues measured photopotential in the absence and presence of oxygen, and their results (submitted/unpublished) indicated that electrons were, indeed, available in the conduction band of VLA TiO_2. The availability of such electrons would usher along Reaction Scheme 1. However, further study is needed to determine the extent of the scheme's role. Regardless, all pathways observed in this study lead to the *m/z* 795.4 fragment, which is free from toxicity produced by the intact Adda amino acid [10]. It is apparent from these pathways that the deviations resulting from VLA-induced NF-TiO_2 photocatalysis continue to maintain fidelity to the removal of the biologically active portion of MC-LR.

3.5. Appearance of observed intermediates

The appearance of intermediates over the course of irradiation in the present study stand in stark contrast to Antoniou and colleague's previous study incorporating ultraviolet light [10]. The previous study observed most products within 2 min of irradiation. On the other hand, in the present study, several intermediates were not observed until several hours of irradiation. The evolution of the appearance of intermediates can be observed in Table 2. It should be noted that although traces of *m/z* 1025.5 appeared prior to 8 h, the signal-to-noise ratio remained slightly below 3:1 until the eighth hour of irradiation.

Another stark contrast to the previous study is the lack of observed attacks on the Mdha amino acid's carbon–carbon double bond. Such intermediates were not observed in the present study. It is possible that a higher initial concentration of MC-LR (Antoniou et al. used 20 ppm), a longer irradiation time (> 8 h), or higher intensity lamp would have presented these intermediates.

4. Conclusions

The degradation intermediates of visible light-induced NF-TiO_2 photocatalysis of MC-LR were identified. Ten peaks corresponding to intermediates appeared, some containing several isomers. One peak was found to be a new intermediate that has not been previously reported according to the authors' knowledge. The new intermediate, however, did not suggest a drastically alternative pathway, but rather fit into a previously established degradation pathway. In total, the numerous intermediates corresponded to three pathways proposed for degradation. All three pathways resulted from attack on the Adda amino acid, and all three produced the same end product, which showed a removal of the biologically active Adda amino acid side chain. Thus, using visible light (e.g., from the sun) to induce NF-TiO_2 photocatalysis to decontaminate waters containing MC-LR continues to be an attractive method.

Acknowledgments

This work was funded by the National Science Foundation US-Ireland CBET (1033317) grant. The authors would like to extend their gratitude to Dr. J. Shoemaker of the United States Environmental Protection Agency for providing mass spectrometry instrumentation used in identifying the intermediates. C. Han is the recipient of the Graduate School Dean's Fellowship, which supports University of Cincinnati doctoral students in their final year of degree work.

Appendix A. Supplementary data

Supplementary data associated with this article can be found, in the online version, at http://dx.doi.org/10.1016/j.apcatb.2014.02.025.

References

[1] Environmental Protection Agency, Fed. Regist 74 (2009) 51850–51862.
[2] B.G. Kotak, A.K.Y. Lam, E.E. Prepas, S.L. Kenefick, S.E. Hrudey, J. Phycol. 31 (1995) 248–263.
[3] H.W. Paerl, J. Huisman, Science 320 (2008) 57–58.
[4] M.G. Antoniou, A.A. de la Cruz, D.D. Dionysiou, J. Environ. Eng. 131 (2005) 1239–1243.
[5] J. An, W.W. Carmichael, Toxicon 32 (1994) 1495–1507.
[6] J.L. Acero, E. Rodriguez, M.E. Majado, A. Sordo, J. Meriluoto, J. Water Supply Res. Technol. AQUA 57 (2008) 371–380.
[7] H. Miao, W. Tao, Sep. Purif. Technol. 66 (2009) 187–193.
[8] K. Harada, K. Tsuji, J. Toxicol.—Toxin Rev. 17 (1998) 385–403.
[9] C. Han, M. Pelaez, V. Likodimos, P. Falaras, K. O'Shea, D.D. Dionysiou, Appl. Catal. B: Environ. 107 (2011) 77–87.
[10] M.G. Antoniou, J.A. Shoemaker, A.A. de la Cruz, D.D. Dionysiou, Environ. Sci. Technol. 42 (2008) 8877–8883.
[11] A. Fujishima, X. Zhang, D.A. Tryk, Surf. Sci. Rep. 63 (2008) 515–582.
[12] C.S. Turchi, D.F. Ollis, J. Catal. 1221 (1990) 178–192.
[13] M. Pelaez, P. Falaras, V. Likodimos, A.G. Kontos, A.A. de la Cruz, K. O'Shea, D.D. Dionysiou, Appl. Catal. B: Environ. 99 (2010) 378–387.
[14] M. Yuan, M. Namikoshie, A. Otsuki, K. Rinehart, K. Sivonen, M.F. Watanabe, J. Mass Spectrom. 34 (1999) 33–43.
[15] I.K. Konstantinou, T.A. Albanis, Appl. Catal. B: Environ. 49 (2004) 1–14.